Clim Dyn (2017) 49:3363–3381
DOI 10.1007/s00382-016-3518-4

Simultaneous modulations of precipitation and temperature extremes in Southern parts of China by the boreal summer intraseasonal oscillation

Yang Chen[1] · **Panmao Zhai**[1]

Received: 8 August 2016 / Accepted: 28 December 2016 / Published online: 24 January 2017

Abstract The boreal summer intraseasonal oscillation (BSISO), including a 30–60 day component (BSISO1) and a quasi-biweekly component (BSISO2), is the most prominent form of subtropical intraseasonal variability. Influences of BSISOs on summertime precipitation and temperature extremes in China are examined. Results indicate that BSISOs can simultaneously facilitate precipitation extremes in central-eastern China and extreme high temperatures in South China-Southeast China. During phase 2–4 of active BSISO1, accompanying precipitation extremes in central-eastern China, there is a fourfold-fivefold increase in probability of extreme high temperatures in Southeast China. About 50% of such simultaneous extremes fall into phase 2–3. BSISO2's influences are pronounced from phase 6 to the next phase 2, with about 58% simultaneous extremes clustered within phase 7 to the next phase 1. It is the BSISO-induced vertical cell, with ascending motion in the Yangtze-Huai River Valley and descending motion in the south, that contributes to simultaneous extremes. Enhanced low-level southwesterlies convey moist and warm air towards southern parts of China. Strengthened ascending branch loaded by anomalously abundant moisture produces precipitation extremes in the north. Concurrently, combined effects of warm advection and descent-triggered adiabatic heating anchors extreme high temperatures well located in South China. The northeastward propagation of the BSISO1 confines influenced regions to eastern-southeastern parts of China, with gradually narrowing spatial extents. The BSISO2-induced simultaneous extremes sweep much broader areas, from southeast coasts to the central inlands. Above analyses on BSISOs-simultaneous extremes relationship lay a crucial scientific basis for predicting these high-impact events on sub-seasonal to seasonal scales.

Keywords Intraseasonal oscillation · Simultaneous extremes · Vertical circulation cell

1 Introduction

It has been well-acknowledged that intraseasonal oscillation (ISO) is an important component of large-scale circulations in both the tropics and subtropics (Madden 1986; Chen and Chen 1993, 1995). The Madden-Julian oscillation (MJO) is a typical manifestation of tropical ISOs (Madden and Julian 1971, 1972). Since the MJO was introduced by Madden and Julian (1971), numerous follow-up studies have investigated its influences on weather and climate anomalies/extremes in various regions (e.g. Zhang 2005; Jones et al. 2004a, b; Alvarez et al. 2016). Specifically, although major activities are confined to equatorial regions, the MJO can still exert indirect impacts on weather anomalies in the extratropics, through exciting diabatically-forced Rossby wave (Matthews et al. 2004). Given much stronger magnitude of MJO cycles within boreal winter, influences of the MJO on weather anomalies are far more pronounced during cold seasons (Madden and Julian 1994; Jia and Yang 2013; Pullen et al. 2015; Jacques-Coper et al. 2015a).

During boreal summer, the ISO is characterized by more complicated propagations and could move off the equator into the subtropics, most notably in Asian monsoonal regions (Wang and Rui 1990, Hsu and Weng 2001;

✉ Panmao Zhai
pmzhai@cma.gov.cn

[1] State Key Laboratory of Severe Weather, Chinese Academy of Meteorological Sciences, CMA, No. 46, South Ave. Zhong-guan-cun, Haidian, Beijing 100081, China

Mao et al. 2010). These northward-progressive ISOs are referred to as boreal summer intreaseasonal oscillation (BSISO), mainly consisting of a quasi-biweekly agent and a 30–60-day agent (Mao and Chan 2005). The biweekly agent exhibits marked northward/northwestward propagation, while the 30–60-day oscillation shows prominent northward/northeastward progression (Waliser 2006; Chu et al. 2012; Jia and Yang 2013). Inspired by the famous MJO index (Wheeler and Hendon 2004), Lee et al. (2013) constructed BSISO indices to achieve purposes of real-time detection, monitoring and prediction of BSISOs. Derived BSISO indices show excellent performances in portraying distinctive periodicities and propagation routes of different agents (Hsu et al. 2016). In sharp contrast to indirect impacts of the MJO on subtropical weathers, BSISO-induced circulation-convection pairs could invade into the subtropics, directly alter local background circulations, and further trigger weather anomalies or even extremes there (Yang et al. 2010; Oh and Ha 2015). For instance, the BSISO could manipulate the onset/end timing and active/break spells of East Asian summer monsoon, which could largely determine summertime temperature and precipitation in China (Annamalai and Slingo 2001; Zhou and Chan 2005; Ding and Chan 2005). Summertime precipitation in the Yangtze River Valley is most sensitive to BSISO activities, especially during Mei-Yu season (Lau et al. 1988; Yang et al. 2010; Li et al. 2015). The BSISO influences on precipitation in the Yangtze River Valley are fulfilled via modulating the position of the western Pacific subtropical high (Ren et al. 2013; Lu et al. 2014). Precipitation extremes also show close relationship with two BSISO components (Hsu et al. 2016; Gao et al. 2016). For instance, both Lu et al. (2014) and Zhu et al. (2003) revealed that floods in the Yangtze River Basin during 1998 were in tandem with the active phase of 30–60-day BSISO. Liu et al. (2014) emphasized the great contribution of the quasi-biweekly agent to heavy rainfall in the Yangtze-Huai River Valley during 2003. Studies based on specific cases can't fully address influences of the BSISO on precipitation extremes in China. Further examination of statistical relationship between each BSISO agent and precipitation extremes is warranted.

Extreme high temperature/heatwave is another type of high-impact events during summer in China (Sun et al. 2014). There exist numerous studies focusing on modulation of extreme temperatures by the MJO during boreal winter (Jacques-Coper et al. 2015b; Matsueda and Takaya 2015). During boreal summer (very weak MJO signals), however, little have hitherto been known about influences of different BSISO agents on temperatures, especially on extreme high temperatures (Chen et al. 2016; Wang et al. 2016). In particular, in the same context of intraseasonal oscillation, temperature extremes and precipitation extremes may occur concurrently in adjacent regions (Chen et al. 2017). The anomalous weather in 2010, with an unprecedented heat wave in western Russia and a devastating flood in Pakistan, is typical of such simultaneous extremes (Galarneau et al. 2012). In fact, these simultaneous extremes are of much greater disaster-causing potential, owing to their great intensity and extensive spatial coverage. Considering BSISO's organized structure with alternative cyclones and anticyclones along propagating routes (Lee et al. 2013), some studies have assessed the potential of these contiguous wave-like cells in inducing opposite precipitation variations in neighboring regions (Tsou et al. 2005; Mao and Chan 2005). Yet comparatively little work has been done to connect different types of extremes in this context. In other words, the question of whether BSISOs and which agent can simultaneously modulate precipitation and temperature extremes in southern parts of China is an interesting yet an open issue remaining to be answered.

This study, therefore, attempts to narrow aforementioned gaps about impacts of BSISOs on extremes in China. Specifically, occurrence probabilities of extreme precipitation and temperature events during active and inactive BSISOs would be compared, and phases most conducive to these extremes should be confirmed. Mechanisms for connecting precipitation extremes and temperature extremes in adjacent regions need to be addressed. The BSISO is believed to be a primary source of predictability of East Asian summer monsoon (Lee et al. 2013, 2015). Taking advantages of quasi-periodicity of BSISOs may promote the extended-range forecasts of extremes. Extension of forecast lead time for high-impact weathers are of high practical value in disaster mitigation and risk management in various societal sectors.

In the next section, data and method are briefly introduced. Section 3 will investigate modulations of extreme temperature and precipitation events by the BSISO, and illustrate responsible mechanisms. Derived conclusions and further discussions would be presented in Sect. 4.

2 Data and method

2.1 Data

To delineate BSISO activities, BSISO indices developed by Lee et al. (2013) are adopted in this study. These indices are constructed via the first four empirical orthogonal functions (EOFs) of combined fields of outgoing longwave radiation (OLR) and 850-hPa zonal wind anomalies over the Asian summer monsoon region [10°S–40°N, 40°E–160°E]. The first agent (BSISO1) is constituted by the first and second EOF principal components, and represents northward/northeastward propagating oscillations

that cover periodicities between 30 and 60 days. The second component (BSISO2) contains joint signals of the third and fourth EOF modes, and captures the feature of northward/northwestward migration of the 10–30-day oscillations. Each BSISO cycle is divided into eight phases, among which the 8th phase is followed by the 1st phase of the next cycle. The extracted BSISO indices are not subject to any band-pass filtering processes. So they can serve the purpose of real-time monitoring and prediction of the BSISO. The BSISO indices over the period from 1981 to 2010 are gained online at http://www.apcc21.org/eng/service/bsiso/moni/japcc030602.jsp.

Weather extremes in China are identified based on an observational dataset including 756 stations. Variables used in this study include daily precipitation, daily mean temperature, daily maximum temperature, and daily minimum temperature during 1981–2010. Before being released, this dataset went through rigorous quality control procedures by the Climate Data Center (CDC) of the National Meteorological Information Center (data and documents available online http://cdc.cma.gov.cn/home.do), China Meteorological Administration (CMA). Extreme precipitation and extreme high temperature mainly concentrate during the period from May to August in southern parts of China, due to influences of East Asian summer monsoon (Ding and Chan 2005; Hsu et al. 2016). So May–August is selected as the study period.

Daily reanalysis data from 1981 to 2010, including geopotential height (gpm), horizontal wind (m/s), specific humidity (kg/kg), air temperature (K), are gained from the National Centers for Environmental Prediction and National Center for Atmospheric Research (NCEP/NCAR), at a horizontal resolution of 2.5°×2.5° (NCEP/NCAR R1, Kalnay et al. 1996). To utilize multi-level specific humidity, the NCEP/NCAR R1, rather than NCEP-2 reanalysis (the National Centers for Environmental Prediction (NCEP)/Department of Energy (DOE) Reanalysis 2, Kanamitsu et al. 2002) is adopted. The ERA-interim reanalysis data (Dee et al. 2011) from 1981 to 2010 is also used to validate composited results via the NCEP/NCAR reanalysis. Composited circulation anomalies from the NCEP/NCAR R1 and the ERA-interim show highly similar patterns (figure not shown), so only the results based on NCEP/NCAR R1 are presented in the following sections.

2.2 Method

Composites of precipitation, temperature and circulation anomalies are computed for each of the eight phases of active BSISOs. Differences of composited variables during active and inactive BSISOs are also calculated. An active BSISO event is considered when corresponding BSISO index exceeds 1 standard deviation, while an inactive BSISO event refers to the day with indices of both BSISO1 and BSISO2 below 1 standard deviation. Inactive BSISOs exhibit somewhat irregular propagating, loosen organized and weak circulation anomalies.

An extreme precipitation (temperature) event is defined as a day with daily precipitation (temperature) above its long-term (1981–2010) 90th percentile. The threshold of extreme precipitation is calculated empirically from the sample of all rainy days during a base period, over a 29-day window centered on each calendar day during May to August during 1981–2010 (Tencer et al. 2014). Instead of the 75th percentile recommended by Tencer et al. (2014) for trend analyses, the 90th percentile is adopted to accentuate high impacts of identified cases. For temperature threshold, as recommended by Expert Team on Climate Change Detection and Indices (ETCCDI), a 5-day window is rationally applied because temperature is a much smoother variable (Zhang et al. 2011; Tencer et al. 2014). We defined temperature extremes based on daily mean temperature, daily maxima and daily minima, respectively, and further evaluate influences of the BSISO on them. Based on our sensitive experiments, slight adjustments of sample window length (e.g. 31-day for precipitation and 7-day, 9-day for temperature) didn't change subsequent results significantly. Such varying daily-based percentiles behave more efficient in identifying extremes during different summer stages; while, a fixed monthly or seasonal percentile reflects more about extremes during peak summer, especially for temperature (Kuglitsch et al. 2010). In spite of slightly lower intensity, early summer extremes may be equally or even more devastating than events during mid-late summer, because people had few opportunities to get themselves prepared to sudden extremes at so early stages (Hajat et al. 2002).

Daily anomalies of atmospheric variables are calculated following the method introduced by Hart and Grumm (2001). Considering possible unequal variances of the extremes-related fields and climatology (Chen and Zhai 2014), both ordinary Student's t test and Welch's t test (Welch 1947) are employed to achieve more rigorous statistical significance. Composited anomalies satisfying higher criteria at the 0.05 level are deemed statistically significant. A bootstrap procedure developed by Efron and Tibshirani (1994) is conducted to estimate the significance level of occurrence probability of extremes during active BSISOs against inactive days. This bootstrap method repeatedly re-sample (1000 times) the record to determine the distribution difference of extremes during a particular phase of active BSISOs relative to that in inactive BSISOs, at each station. If the average frequency difference is higher than the 95th percentiles of the difference in total repetitions, it is recognized that the occurrence probability of extremes is significantly higher (at the 0.05 level) during

active BSISOs. Such bootstrap method was widely used in existing studies to evaluate significance of extreme event frequency during active MJO phases (e.g. Bond and Vecchi 2003; Matsueda and Takaya 2015). For each station, if both the probability of extreme precipitation (temperature) and composited mean precipitation (temperature) is significantly higher during active BSISOs, it is referred to as a '*significant station*'.

3 Results

3.1 BSISO1-extremes

Figure 1 displays changes in occurrence probability of precipitation extremes (left column) and temperature extremes (right column) during active BSISO1 against inactive days. Modulation of precipitation extremes by active BSISO1 shows obvious location preference, with significantly elevated probability mostly situated in the Yangtze-Huai River Valley (YHRV, 112.5–125°E, 28–32°N). During Phase 1, significant increases of probability can be found in only a few stations in the YHRV (Fig. 1a, filled dots). During Phase 2–4, the spatial extent of significantly increased probability expands substantially, covering almost the entire YHRV and lower reaches of the Yangtze River. Most stations within these regions observe a doubling or even tripling of occurrences of precipitation extremes during active BSISO1 days. After Phase 5, regions recording significantly increased probability shrink rapidly. As the BSISO1 cycle continues to evolve, a mirror pattern of extreme precipitation occurrence takes shape gradually, but with several exceptive stations along southeast coast still seeing significantly increased probability during Phase 7–8. The most obvious influences of BSISO1 on temperature extremes occur during Phase 1–3, in South China-Southeast China. More specifically, during Phase 1, extreme high temperatures tend to occur in Hainan Island and coastal areas in South China. Subsequently, significant increases in probability appear across Southeast China, with increased percentage of 60–130%. Of particular note is that Fig. 1 only shows influences of BSISO1 on extremes of daily maximum temperature. Occurrence probability of extremes based on daily mean temperature and daily minimum temperature don't show significant differences between active and inactive BSISO1 (figure omitted). Some stations in South China-Southeast China even observe reductions of temperature extremes of daily mean and minima during active BSISO1. The reason for this phenomenon would be explained in the following analyses.

It seems that Phase 2–3 of the BSISO1 could simultaneously elevate the chance of precipitation extremes in the YHRV and high temperatures in the south. To confirm such simultaneous modulation, we further examine occurrence probability of extreme temperature (precipitation) events, when BSISO1-related extreme precipitation (temperature) events surely occur in the YHRV (South China-Southeast China). Following the method introduced by Chen and Zhai (2013), a BSISO1-related extreme precipitation event is considered when at least three neighboring significant stations ('significant station' please refer to Sect. 2.2) in the YHRV register precipitation extremes during a day of active BSISO1. Distance between neighboring stations is required to be less than 20 km, which is the representative radius of each station in this observational network Spatial extent enclosed by at least three stations effectively eliminates small-scale local convections. Adoption of significant stations further ensures the significant connection of active BSISO1 and identified extreme events. Most (above 90%) identified BSISO1-related extreme precipitation events appear during Phase 2–4, consistent with the result shown in Fig. 1. It needs to be firstly clarified that during identified days, precipitation extremes definitely occur within the YHRV, but not necessarily in every station. As shown in Fig. 2a–c, during these identified days, the probability of extreme precipitation in some stations can reach 30% or greater (with the maximum of 57%); while during inactive BSISO1 days, the probability is about 5–7% in this region. Accordingly, there is a threefold to fivefold increase in occurrence of precipitation extremes in most stations, and the maximum increase is beyond sevenfold. In most stations in South China-Southeast China, extreme high temperature days account for 6–8.5% in total inactive BSISO1 days. However, accompanied by BSISO1-related extreme precipitation in the YHRV, probability of extreme high temperature grows tremendously in the south, with the highest occurrence probability up to 55% (Fig. 2d–f). When precipitation extremes occur in the YHRV, the occurrence probability of extreme high temperatures in South China-Southeast China grows by a factor of 4–5. In a similar way, when BSISO1-related extreme high temperature events occur in South China-Southeast China, occurrence probability of precipitation extremes in the YHRV can reach 20–25%, an approximate threefold increase than the probability during inactive BSISO1 (figure not shown). However, significant stations of temperature extremes are far less than significant stations of precipitation extremes (Fig. 1). So the number of BSISO1-related extreme temperature events is much smaller. To guarantee enough cases for assessing significance, only the situation during BSISO1-related extreme precipitation events are shown here and in the following parts.

Above analyses confirm the potential of the BSISO1 in simultaneously modulating precipitation extremes and temperature extremes in adjacent regions. The intensity of these concurrent extremes is intuitively displayed in

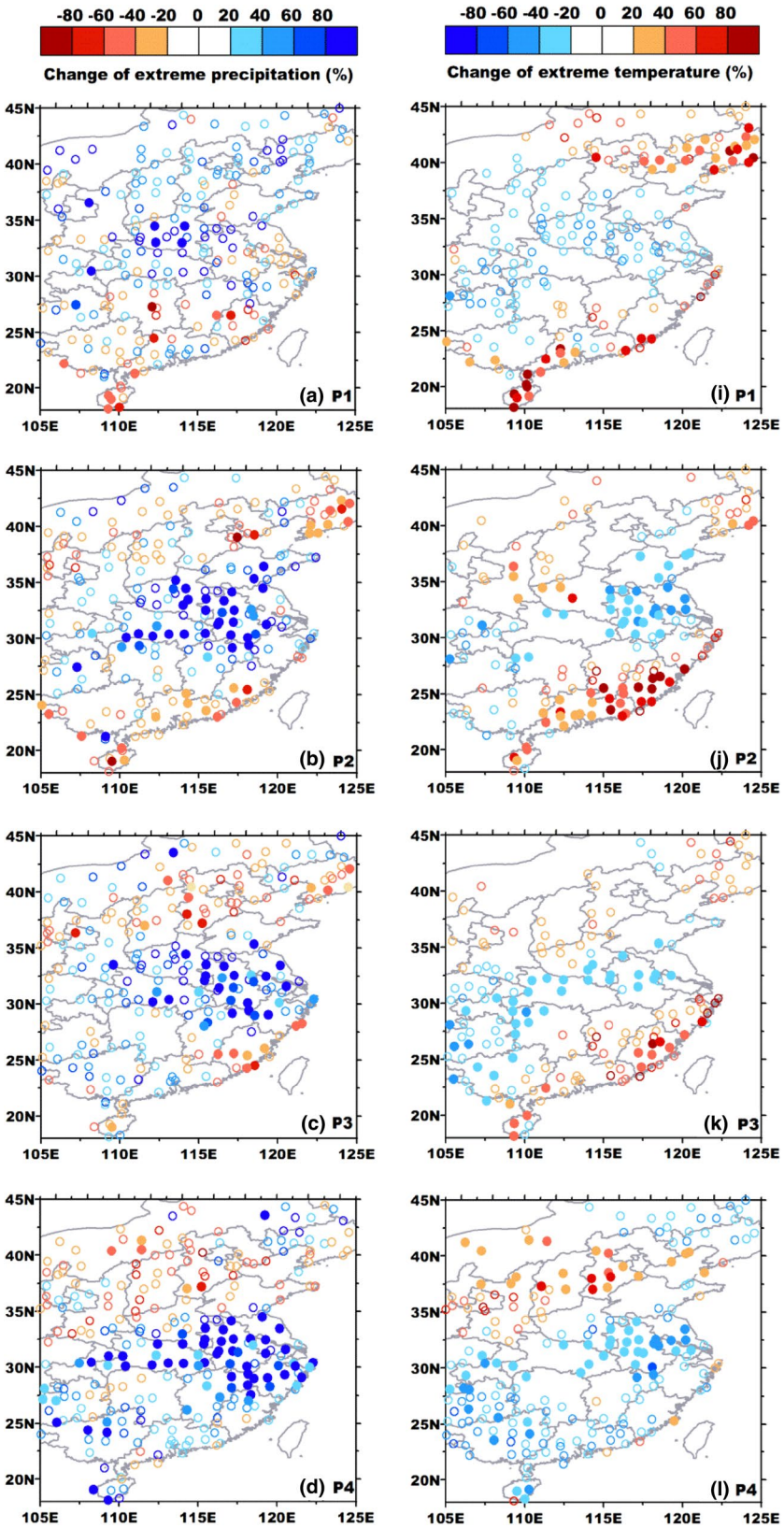

Fig. 1 Percentage changes (%) in occurrence probability of precipitation extremes (*left column*) and extremes of daily maximum temperature (*right column*) during active phases of the BSISO1 against inactive BSISOs. Following the method introduced by Hsu et al. (2016), for phase-i, the percentage change is calculated as $\frac{[P_{active(i)} - P_{inactive}]}{P_{inactive}} \times 100\%$, in which $P_{a(i)ctive}$ represents occurrence probability of extremes during all days of active phase-i, and P_{active} stands for occurrence probability of extremes during all days of inactive BSISO1. For each phase, significant stations are highlighted by *shaded dots*. Here, significant stations record significantly higher probability of extremes and significantly higher precipitation/temperature during active BSISO1 in relative to inactive BSISO1. Letter *P* in the *lower-right corner* of each figure represents word 'phase'

Fig. 1 (continued)

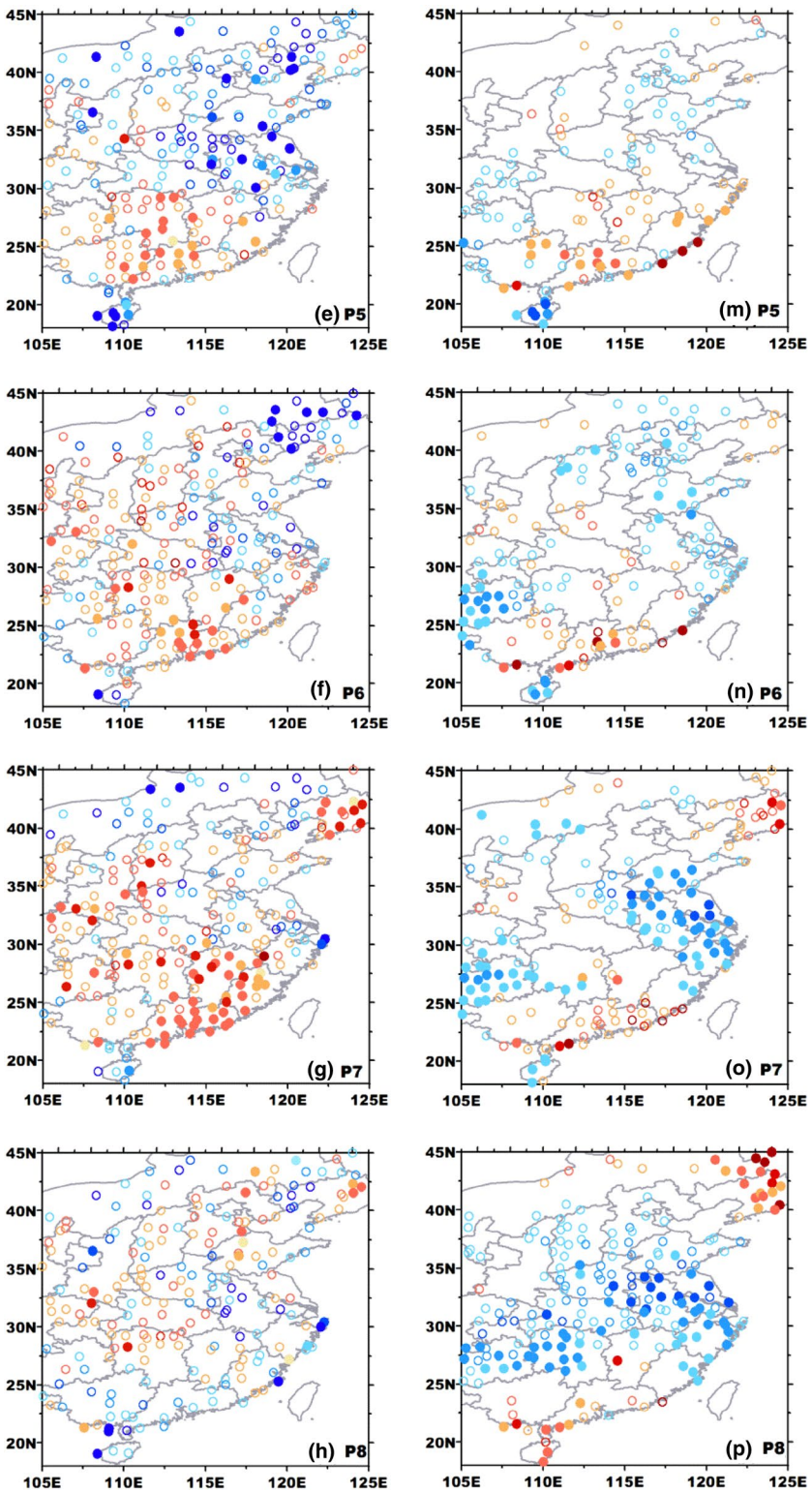

Fig. 3a–c. Composited precipitation for BSISO1-related extreme precipitation events can reach 35 mm day^{-1} or greater, equivalent to 3–5 standard deviations above normal. Meanwhile, in South China, daily maximum temperature exceeds 35 °C or even 37 °C, exceeding 2 standard deviations above climatological mean. The BSISO1-related anticyclone plays a key role in triggering simultaneous extremes. During Phase 2, the anomalous anticyclone resides in the north of the Philippines. During Phase 3–4, this anticyclone moves northeastward off the mainland

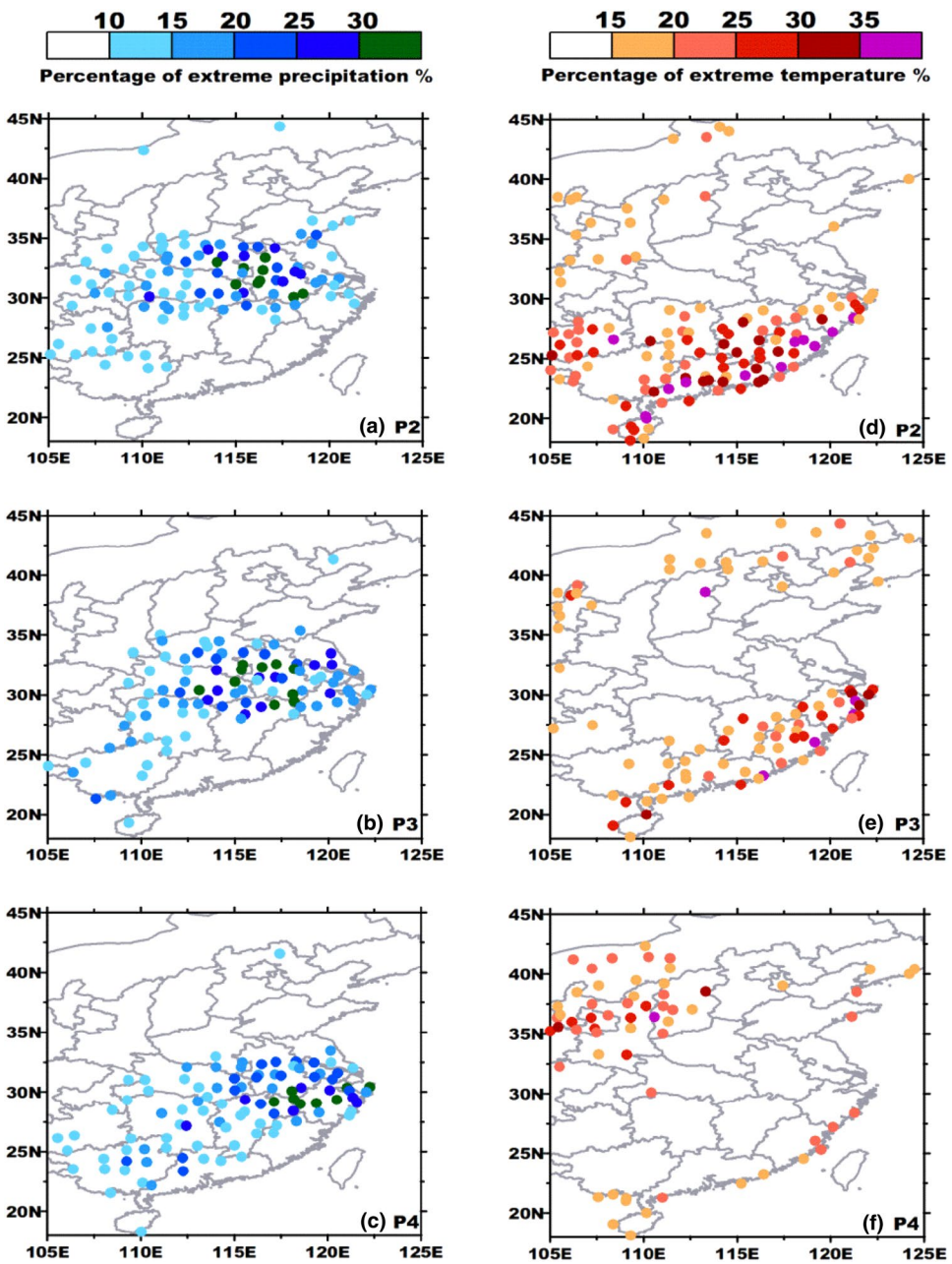

Fig. 2 Occurrence probability of extremes of precipitation (*left column*) and daily maximum temperature (*right column*) during BSISO1-related extreme precipitation events in Phase 2–4 (see Sect. 3.1). Letter *P* in the *lower-right corner* of each figure represents word 'phase'

China, arriving at south of Japan. Such northeastward migration is typical of BSISO1 activities, and determines eastward extension of extreme precipitation in the YHRV and the contraction of high temperature zone in the south. In essence, this BSISO1-related anomalous anticyclone induces position anomalies of the western Pacific subtropical high (WPSH), which is a key system responsible for anomalously abundant moisture required by precipitation extremes in the YHRV (Chen and Zhai 2014). As exhibited in Fig. 3a–c, in response to the northeast propagation of the anticyclone, the WPSH (1490gpm-contour at 850 hPa) retreats southeastward gradually. A BSISO1-related vertical circulation cell, with ascending motion around the YHRV and descending motion around South China, serves as a medium connecting precipitation extremes in the north and temperature extremes in the south. In the lower troposphere (below 500 hPa), enhanced southerlies/southwesterlies in the northern flange of WPSH advects abundant moisture towards the YHRV (blue contours in Fig. 3d–f). These moist southerlies/southwesterlies converge with northerlies from mid-high latitudes, contributing to strong ascending motion and heavy precipitation in the north. The northward tilted ascending motion is indicative of typical frontal structure, in tandem with large spatial scale of resulting precipitation (Chen and Zhai 2015). Released strong diabatic heating in the mid-high levels favors upper level divergences,

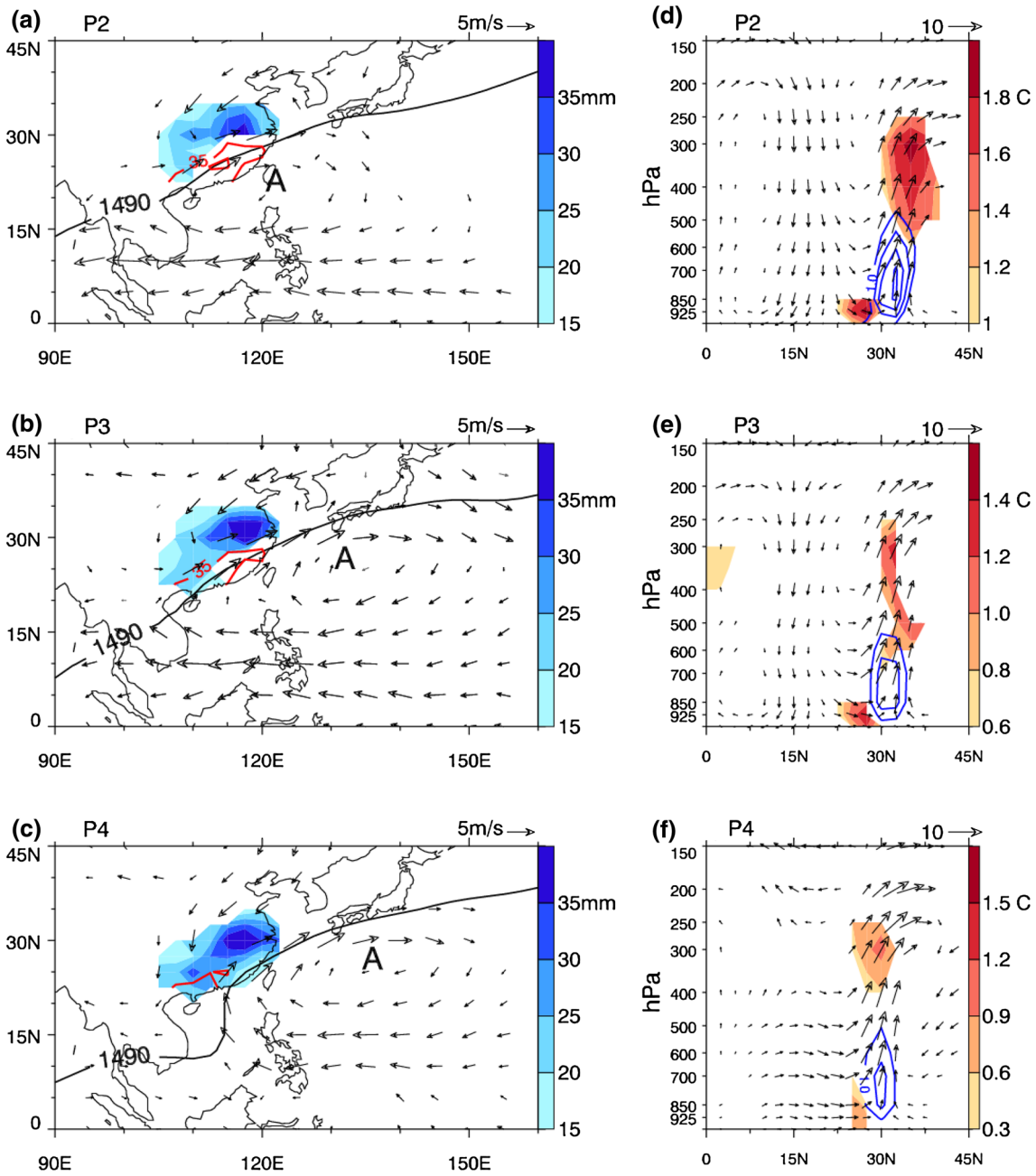

Fig. 3 Composited precipitation (mm day^{-1}, *shadings*), temperature (°C, *red contours*), 850 hPa wind anomalies (m s^{-1}, vectors) and 1490gpm-contour (*black contour*) for the western Pacific subtropical high are displayed in (**a**–**c**). Only wind anomalies significant at the 0.05 level are shown, and vectors in the regions higher than 850 hPa are blocked. Letter *A* generally labels the center of the anomalous anticyclone. **d–f** shows pressure-latitude cross [averaged within 115°E–120°E] of temperature anomalies (*shadings*), specific humidity anomalies (k kg^{-1}) with contour interval of 1.0 k kg^{-1}, wind anomalies (vectors, v component-m s^{-1}, ω component- −0.01pa s^{-1}). Only significant anomalies are shown in (**d**–**e**). To focusing on our target area, only temperature anomalies north of 17.5°N are presented. Letter *P* in the *lower-right corner* of each figure represents word 'phase'

exciting a northerly return flow atop South China. Low-level divergences caused by the anomalous anticyclone force strong descending motion that prevails atop the South China Sea to Southeast China. These descending flows dissipate widespread clouds there, so more solar radiation can heat the surface. Likewise, adiabatic heating from descending motion also contributes to the elevated temperature in the lower-levels (Fig. 3d–f). What is worth noting is that the strongest warming anomaly in the lower troposphere is well anchored in South China, rather than over the region with

strongest descending motions. It seems incompatible with above statement about essential role of adiabatic heating. Further budget anatomy of temperature equation (figure omitted) indicates that in addition to decent-related adiabatic heating, southwesterly-induced warm advection plays an equally-important role in constructing above unique warming pattern. So it is the BSISO1-induced vertical circulation cell that gives rise to simultaneous extremes in southern parts of China, in both a dynamical and thermodynamical way. As the BSISO1 departs from China, the vertical cell slowly retreats southward accordingly. During Phase 4 when the main body of anomalous anticyclone displaces far away from South China, the vertical cell vanishes (Fig. 3f), although extreme precipitation still exists in the south of the Yangtze River. At this stage, with the absence of adiabatic heating, warm anomalies caused by warm advection are characterized by weaker magnitude and smaller spatial scale. So the descending motion and accompanying hot weather are not simple passive responses to extreme precipitation in the north. Instead, the activity of BSISO1 is the determinant in establishing the vertical cell and exciting simultaneous extremes. During nighttime, in the context of decent-induced clear sky, the heating is partly offset or even exceeded by cooling caused by increasing outgoing longwave radiation from the surface. So daily minimum/mean temperature fail to evolve into high temperature extremes.

3.2 BSISO2-extremes

Modulated by active BSISO2, spatial patterns of extreme precipitation and temperature events obviously differ from those associated with BSISO1. Significant influences of BSISO2 on precipitation extremes span from Phase 5 to Phase 8, and continue onward to Phase 1–2 of the next cycle. During Phase 4, stations with increased probability of precipitation extremes start to emerge along coastal regions of Southeast China. Afterwards, significant stations rapidly shift northwestward to the inland area. Generally, during active BSISO2, percentage increases of precipitation extremes in these areas range from 50 to 120%. Till Phase 1, significant stations march northward as far as in central part of China. For extreme temperature events, stations with percentage increases above 50% are distributed along southeast coastal regions during Phase 6. Subsequently, regions seeing significant increased occurrences of temperature extremes expand westward obviously and northward slightly. Particularly, during active Phase 1, significant stations of temperature extremes cover large parts of South China-Southeast China, with occurrence probability doubles that during quiescent BSISO2. It seems that the BSISO2 can also simultaneously modulate occurrences of precipitation extremes and temperature extremes, especially during Phase 6 to the next Phase 2.

Following the method for BSISO1-extreme precipitation events, we also identified BSISO2-related extreme precipitation (temperature) events, and further examined simultaneous occurrences of extreme temperature (precipitation) events. According to Fig. 4, the target area for identification of precipitation extremes during Phase 6–8 is still selected as [112.5–125°E, 28–32°N]. Considering subsequent northwestward advance of the rainbelt, target areas for Phase 1–2 should be also expand northwestward, i.e. [107.5–125°E, 28–35°N]. Similarly, the identified days mean that extreme precipitation events certainly occur within the target area, but not necessarily in each station. During BSISO2-related extreme precipitation events, the probability of precipitation extremes can reach 30% or greater (with the maximum of 61%), far exceeding (a threefold increase) the normal probability in this region (Fig. 5). During these BSISO2-related extreme precipitation days, apart from eastern China, southwest China and middle reaches of the Yangtze River also observe sharply increased occurrences of extreme high temperature. As BSISO2 phase develops, regions with high frequency of extreme high temperatures broaden gradually, in contrast to the narrowing spatial extent of temperature extremes during active BSISO1.

It is can be validated in Fig. 6a–e that the BSISO2 can result in concurrent precipitation and temperature extremes in adjacent regions. During BSISO2, the rainband of extreme precipitation and high temperature zone are more typical of transient ones, not as stationary as those during BSISO1. Such transience easily produces an illusion that influences of BSISO2 on extremes don't vary with evolving phases. By thoroughly inspecting spatial patterns of percentage changes, opposite variations could actually be detected in southern parts of China, especially during phases with well-established cyclonic/anticyclonic anomalies (Phase 1 vs. Phase 5, and Phase 4 vs. Phase 8). The BSISO2-related anticyclone shows swift northwestward migration, and weakens apparently during the propagation. Thus, descending motion governed by the anticyclone behaves weaker than its counterpart during BSISO1. In spite of lower intensity, the anticyclone still boosts northwestward advance of the WPSH and drives the vertical cell to march northward (Fig. 6f–j). Till the next Phase 1, when the center of the anticyclone lands in South China, its intensity drops substantially, with the complete anticyclonic gyre hardly discerned. Therefore, the vertical circulation cell during BSISO2 is characterized by asymmetric structure, with strong ascending branch to the north and reasonably weak descending branch to the south. Similar to the situation of BSISO1, the lower-level warming center over South China is ascribed to joint heating effects of adiabatic descent and warm advection entailed by the

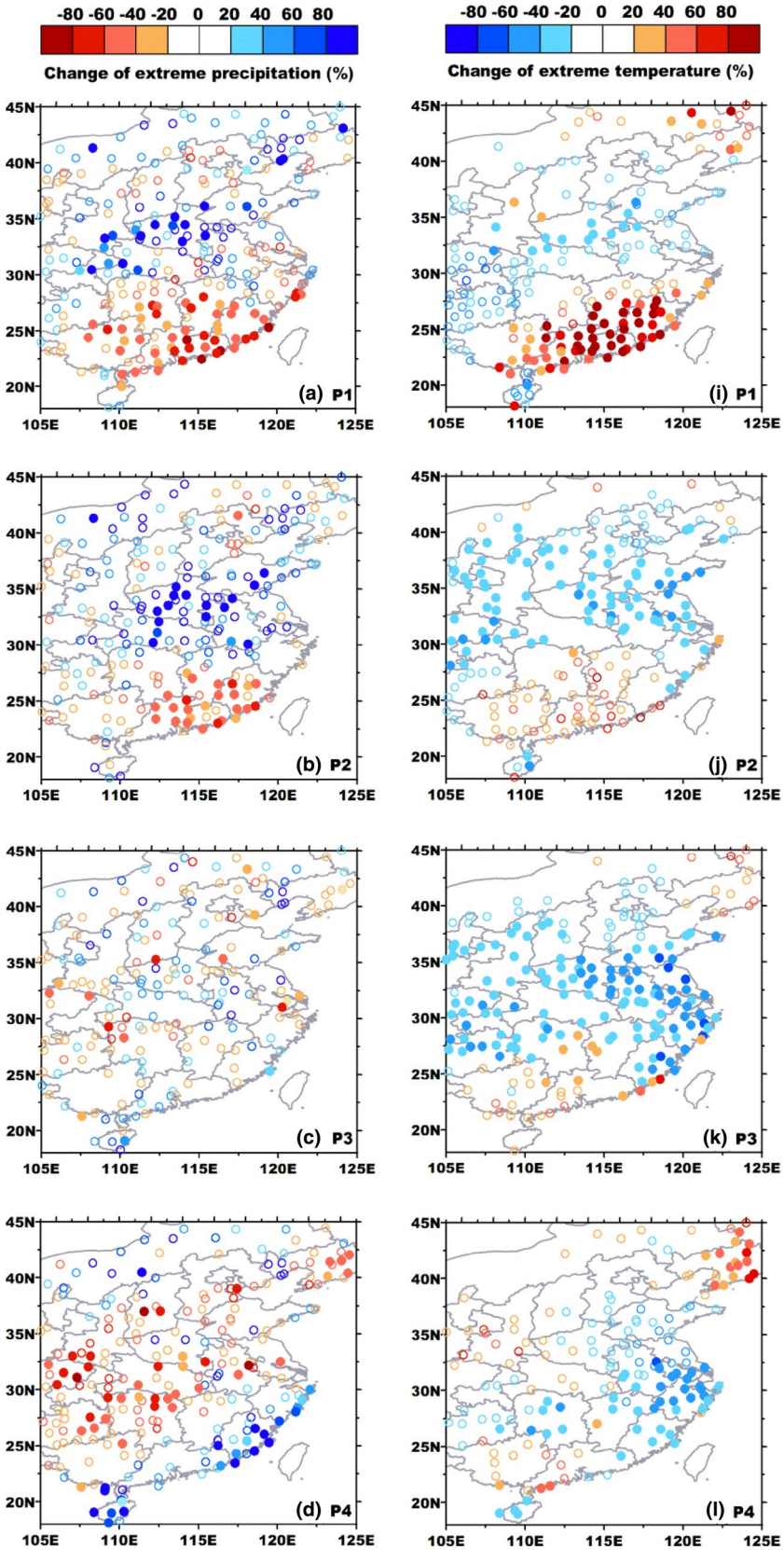

Fig. 4 The same as Fig. 1, but for the BSISO2

Fig. 4 (continued)

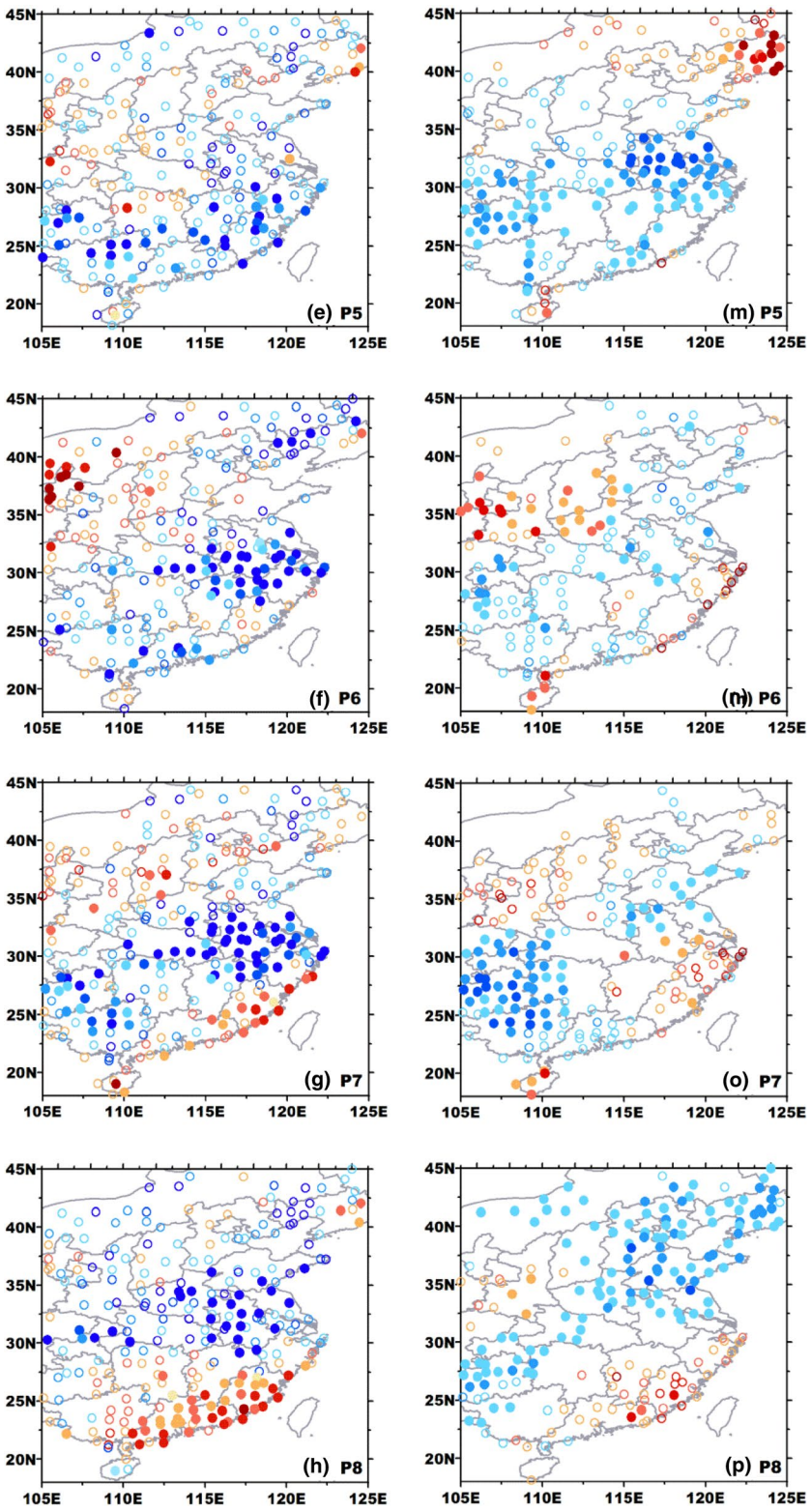

vertical cell. As descending motion strengthens and southwesterly enhances, co-existence of these two heating effects contributes to a strikingly amplified warming center at the lower-levels during phase 8 to the next phase 1. The WPSH arrived at its westernmost point during the next Phase (1) At this stage, almost all regions south of the Huai River are controlled by the WPSH, so the entire southern parts of China witness scorching days.

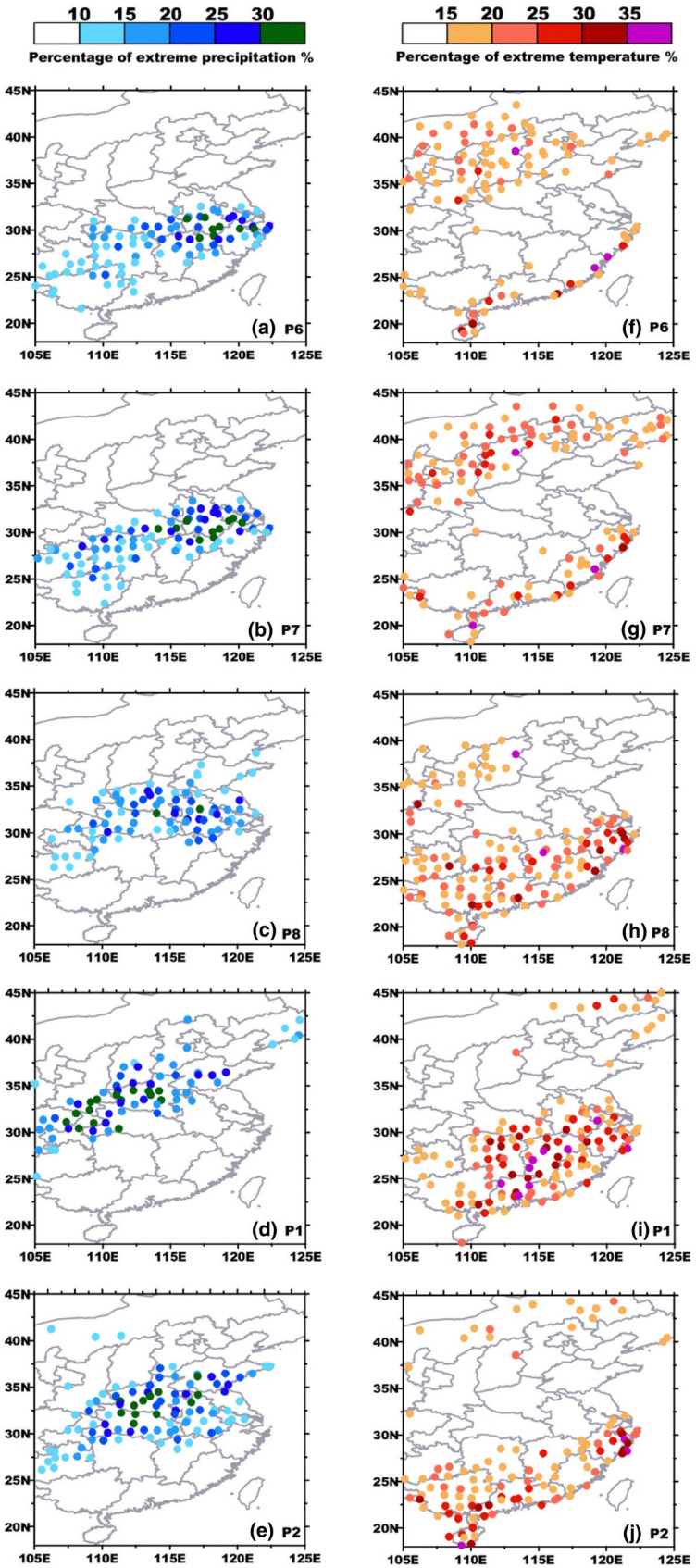

Fig. 5 The same as Fig. 2, but for Phase 6 to the next Phase 2 of the BSISO2

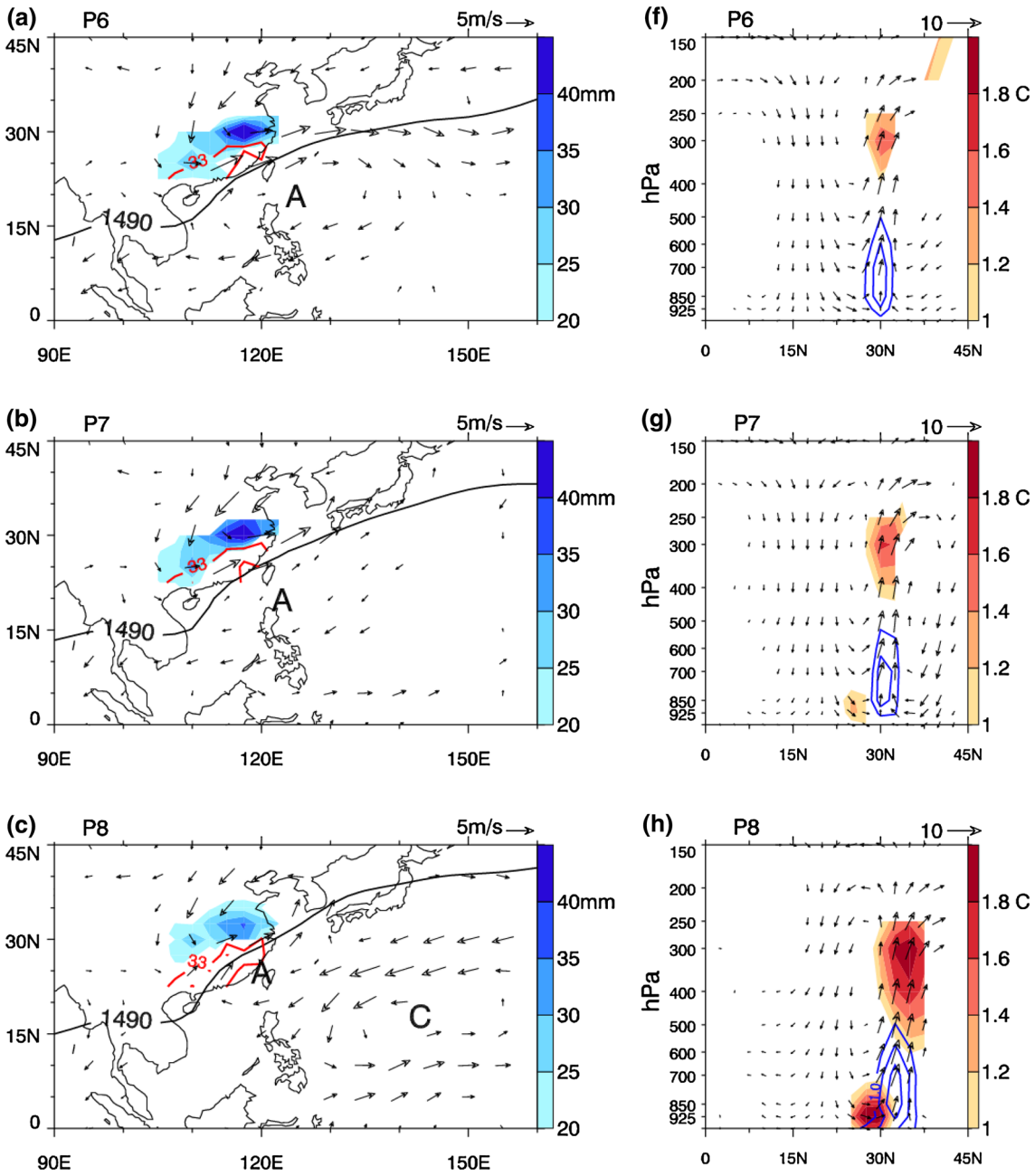

Fig. 6 The same as Fig. 3, but for Phase 6 to the next Phase 2 of the BSISO2

Interestingly, during Phase 6–7, precipitation extremes prevail in the lower reaches of the Yangtze River; however, during the next Phase 1, temperature extremes hit in the same region. Therefore, within about a week from Phase 6 to the next Phase 1 of the BSISO2, the lower reaches of the Yangtze River may alternatively suffer from different extremes. As the anomalous anticyclone dissipates to disappear, descending branch in the south weakens to vanish. So the extreme temperature zone shrinks and displaces southward again (Fig. 6e). Particularly, during the next Phase 1–2, easterlies in the northern flange of the anomalous cyclone, which takes shape since Phase 8 (Fig. 6e), also convey abundant moisture towards the YHRV. The moisture transport via easterly is most pronounced during the next Phase (2) That explains why strong diabatic heating still exists or even further intensifies, in the absence of strong southerly moisture transport (Fig. 6i–j).

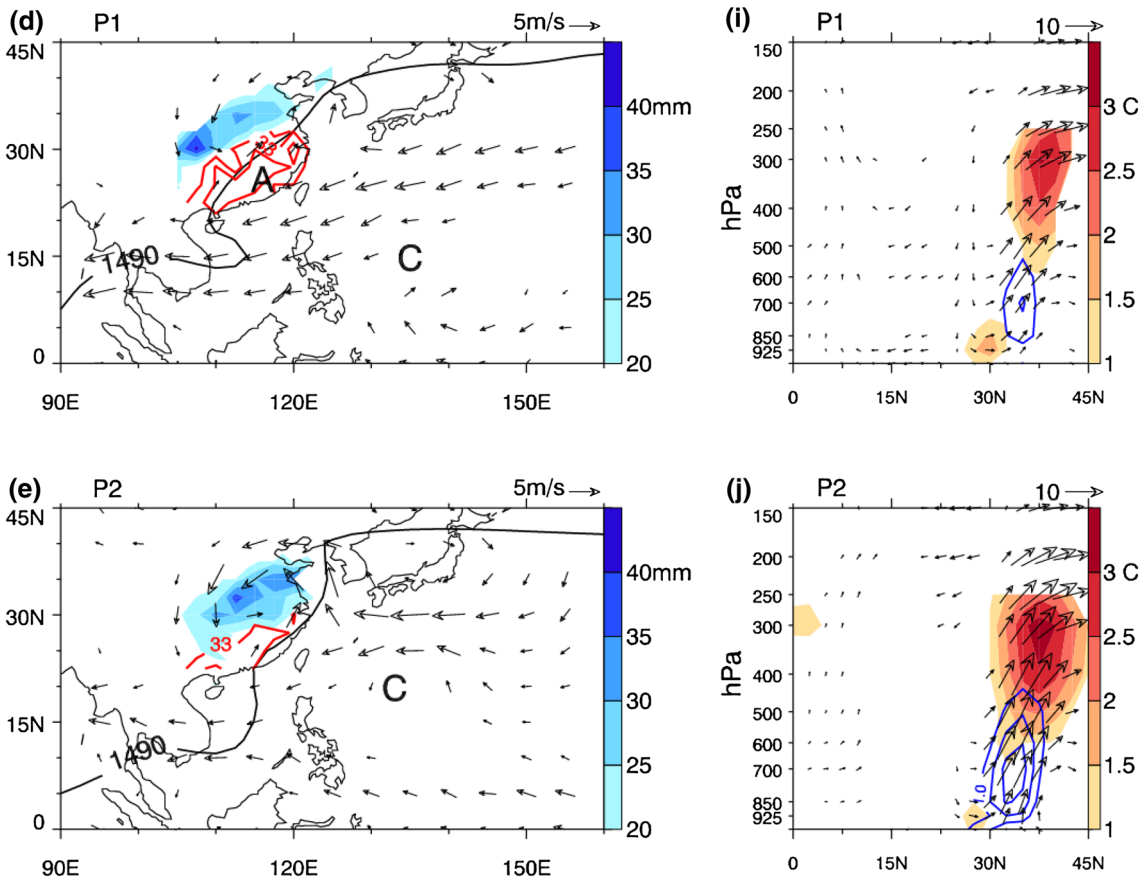

Fig. 6 (continued)

3.3 Favorable phases for simultaneous extremes

The above analyses show that when precipitation (temperature) extremes occur in the YHRV (South China-Southeast China), South China-Southeast China (the YHRV) have a greater chance to register accompanying extreme high temperature (precipitation). This implies great potential of BSISOs in simultaneously modulating different types of extremes in adjacent regions. One may still argue that sharp increases in probability can't ensure actual concurrent occurrences of extremes in the same day.

To address such concerns, we further rigorously defined simultaneous extremes and assessed their dependence on BSISO phases. A simultaneous extreme event is selected when an extreme precipitation event is observed in at least three adjacent stations in northern parts [28–35°N, 112.5–125°E], and in the same day extreme high temperature is recorded in at least three neighboring stations in southern parts [20–28°N, 112.5–125°E].

For the BSISO1, simultaneous extremes during Phase 1–4 account for about 70% of total events during 1981–2010. Particularly, about 50% of simultaneous extremes occur during Phase 2–3. Such phase preference of simultaneous extremes is consistent with high occurrence probabilities presented in Fig. 2a, b. For the BSISO2, simultaneous extremes tend to occur from Phase 7 to the next Phase 1, when 58% events are observed. During inactive BSISOs, the anomalous anticyclone shows random and vague propagations, and its intensity is much weaker. As a consequence, the crucial vertical circulation cell rarely forms in southern parts of China (figure omitted). In this regard, simultaneous extremes falling into phases of inactive BSISOs (within the red circle in Fig. 7) may be more of coincidence, rather than arise from BSISO-related circulation anomalies. Moreover, events associated with active BSISOs far outnumber cases occurring during inactive BSISOs. This is especially true for those favorable phases.

3.4 Comparisons between influences of BSISO1 and BSISO2

Above analyses reveal modulation of extremes by each single BSISO agent, with potential contributions or distractions from the other agent less considered. So it is desirable to address a naturally-raised question that which BSISO component (BSISO1 or BSISO2, or both) is essential for

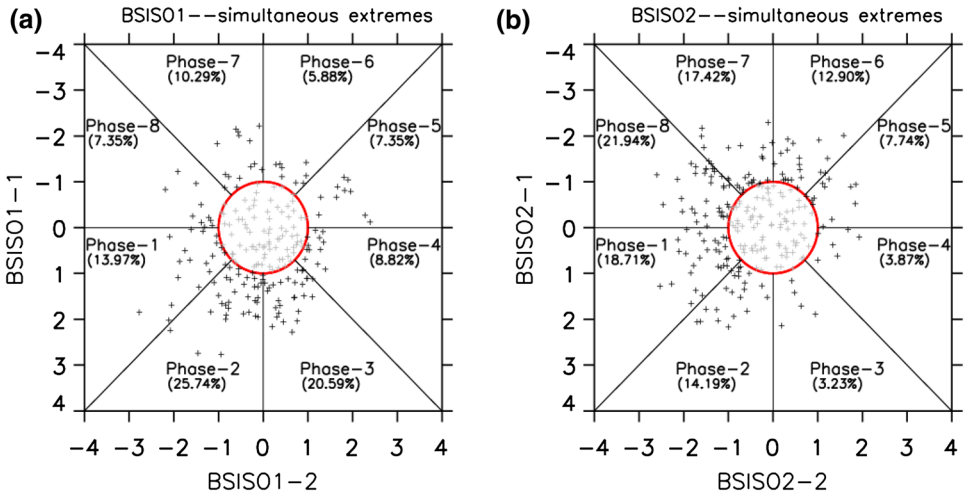

Fig. 7 Phase distribution of simultaneous extremes **a** for BSISO1 and **b** for BSISO2. The percentage of simultaneous extremes falling into each phase is labeled in the bracket. The symbol '+' represent simultaneous extremes, and is located by relevant BSISO indices in *X*-axis and *Y*-axis. The *red circle* frames weak BSISO activities, and the events falling into the *circle* are masked by *light grey color*. (Detailed phase partitions and their concrete meanings may refer to Lee et al. 2013)

occurrences of extreme precipitation/temperature events. Firstly, joint distribution between favorable phases of each BSISO, i.e. BSISO1 phase 2–4 and BSISO2 phase 6-next phase 2, is quantitatively evaluated. Taking phase 2–4 of BSISO1 as an example, most active days in these phases (35–40%) are independent of active BSISO2. Preferred combination largely concentrates within phase 1–2 of BSISO2, with percentages up to 18%. The number of combination with other phases of BSISO2 is very limited, less than 1 day year-1. Secondly, independent influences of each BSISO agent on occurrences of extremes are re-evaluated, with possible interferences from the other component completely removed (e.g. index for phase 2 of BSISO1 $\geq$1.0 and index for all phases of BSISO2 <1.0). Derived results show that even with BSISO2 eliminated, phase 2–4 of BSISO1 are still capable of significantly elevating probability of extremes (figure omitted), with the magnitude of percentage change, affected regions and spatial patterns highly similar to those presented in Fig. 1. Similarly, after removing BSISO1 signals, BSISO2 can still induce extremes in similar regions, with similar percentage changes as shown in Fig. 4. It is therefore reasonable to believe that both BSISO1 and BSISO2 are essential for the occurrence of extreme rainfall/temperature events. Moreover, as indicated by Fig. 3 (6), even with BSISO2 (BSISO1) included, BSISO1-induced circulation anomalies still display obvious northeast (northwest) propagation, consist with their typical propagating routes. Hence, changes in occurrences of extremes shown in Figs. 3, 6 do reflect individual influences of BSISO1 and BSISO2.

Considering possible collaboration of circulation anomalies and commonly-affected location, it seems worth quantifying changes in extreme occurrence during phase 2–4 of BSISO1 with and without phase 6–8 of BSISO2. However, the number of days with combined active BSISO1 and BSISO2 is so limited (less than 20 days during 30 years). Conclusions derived from such a small sample size are not statistically robust enough, especially true for extremes of high randomness and small probability. The small sample size also impairs the significance of circulation anomalies (figure omitted). Weak and insignificant circulation anomalies can't support pertinent conclusions, although it may interestingly show markedly increased probability of extremes during days with certain combined BSISO1 and BSISO2. As stated above, active phases 2–4 of BSISO1 are frequently accompanied by active phase 2 of BSISO2. Nevertheless, circulation anomalies excited by phase 2–4 of BSISO1 are partly cancelled by counterparts induced by phase 2 of BSISO2 (figure omitted). So the configuration between phase 2–4 of BSISO1 and phase 2 of BSISO2 is not conducive to extreme occurrences.

From the perspective of absolute intensity, BSISO1-induced temperature extremes seem stronger than cases associated with BSISO2; while precipitation extremes are slightly severer during BSISO2. One may suspect that composited absolute intensity of extremes may be sensitive to occurrence timing. Inclusion of more peak-late summer days would undoubtedly yield higher temperatures, while more participating days during monsoon season could generate larger amount of composited precipitation. In fact, as indicated by Fig. 8a, occurrence of BSISO-related extremes generally covers the whole summer period, with BSISO1-related events occurring a little earlier. Specifically, nearly 70% of BSISO1-related events occur before July, while the percentage for these early events among BSISO2-related cases is less than 60%. Such timing distribution about seasonality still holds when inspecting occurrence of associated with individual favorable phases. If simply judged by seasonality, the intensity of BSISO1-induced extremes should reasonably be anticipated lower than that of BSISO2-related cases. However, after subtracting seasonal cycle, normalized anomalies behave slightly stronger for

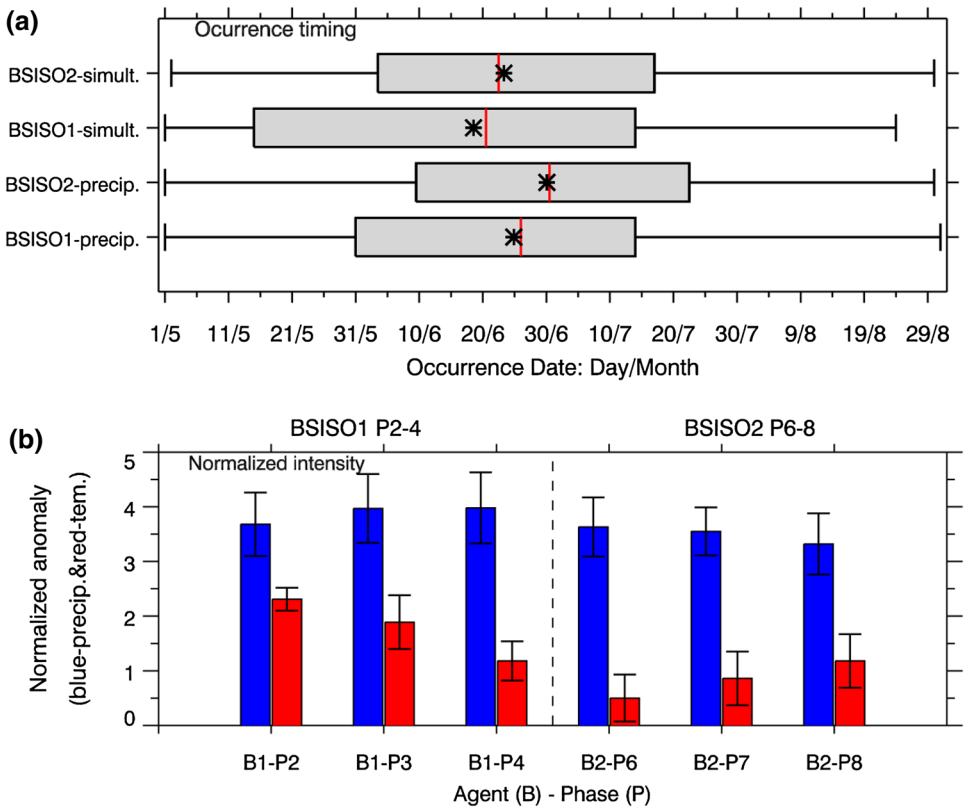

Fig. 8 **a** Box-plot of occurrence timing of extremes associated with different BSISO agents. Five *horizontal bars* indicate the minimum, first quartile, median, third quartile and the maximum respectively. The *asterisk* denotes the mean value. 'BSISO1-precip.' and 'BSISO2-precip.' refer to cases used in Figs. 3, 6 respectively; 'BSISO2-simul.' and 'BSISO2-simul.' include cases used in Fig. 7a, b. **b** Composited normalized anomaly of precipitation (*blue*) and temperature (*red*) in key regions. The domain for temperature anomaly is selected as [112.5–125°E, 20–27°N], and the region for precipitation anomaly is chosen as [112.5–125°E, 28–32°N]. All the anomalies are significant at the 0.05 level, with *error bar* indicating their confidence interval. B1 and B2 refer to BSISO1 and BSISO2 respectively, and *P* denotes 'phase'

precipitation extremes and far more intensified for temperature extremes during BSISO1. That could be explained into that active BSISO1s tend to produce stronger anomalies, regardless of seasonality.

It is difficult to exactly quantify influences of BSISOs on durations (persistence) of extremes. This is because an active BSISO phase is not necessarily preceded or followed by days with active and strong BSISO signals. During these inactive BSISO days, despite occurrence of extremes, its connection with BSISOs can't be guaranteed. Based on real-time BSISO indices, only those extremes accompanied with active BSISO days could be attributable. But anyway, based on an approximate estimation, both temperature and precipitation extremes may persist for 2–3 days on average centered on specific favorable phases, and there are no obvious differences between durations of extremes during BSISO1 and BSISO2.

4 Summary and discussions

4.1 Summary

Numerous studies have reported significant modulation of extremes by low-frequency oscillations, such as the MJO and BSISO. Most of these studies investigated influences on single type of extremes. Focusing the domain of the mainland of China, this study reveals that active BSISOs could induce simultaneous extremes of precipitation and temperature in adjacent regions during summer.

Compared with the situation during inactive BSISO1, probability of extreme precipitation events during phase 1–4 of the BSISO1 increases sharply in the YHRV. Among these favorable phases, risks of extreme high temperature are also heightened apparently in Southeast China during Phase 2–3. When precipitation extremes occur in the YHRV during BSISO1 Phase 2–3, the probability of extreme temperature events in Southeast China increases over fourfold. During Phase 2–3, a BSISO1-related anticyclone excites an anomalous vertical cell, which is constituted by strong ascending motion in the YHRV, upper-level return flow atop South China, strong descending motion in southeast China, and southwesterly moisture transport towards the YHRV. Combined strong ascending motion and abundant moisture convection contribute to extreme precipitation in the north; meanwhile strong descending branch results in increasing incoming solar radiation and adiabatic heating, both of which elevate surface air temperature in the south, especially for daily maximum temperature. The configuration between adiabatic heating and warm advection determines the strongest warming center well-located in South China. So simultaneous extremes happen in adjacent regions in southern parts of China, with about 50% cases falling into phase 2–3.

During active BSISO2, from Phase 5 to the next Phase 2, regions with significantly increased probability of precipitation extremes shift from southeast China to central inland areas. Also northwestward migrated is the zone with higher probability of extreme temperature. During Phase 6–2 of active BSISO2, when extreme precipitation hits the YHRV, regions to the south tend to be scorched by extreme high temperature, with the maximum probability of temperature extremes above 50%. The vertical cell induced by BSISO2 also accounts for simultaneous extremes in adjacent regions, both dynamically and thermodynamically. Phase 7 to the next Phase 1 are the most conductive period for occurrences of simultaneous extremes, totally recording about 60% of all cases during 1981–2010.

4.2 Discussion

Hsu et al. (2016) and Lee et al. (2013) also concluded that Phase 2–4 of the BSISO1 and Phase 5–7 of the BSISO2 are favorable for enhanced precipitation in the Yangtze River Valley. They further composited circulation anomalies during all active days with respect to each favorable phase. However, not every active day within these conductive phases can result in enhanced precipitation, especially for precipitation extremes of small probability (see Figs. 3, 6). Signals of circulations anomalies responsible for precipitation extremes might be largely smeared by non-extreme precipitation days included in normal composites. In contrast, composites in this study are rigorously conducted with respective to BSISO-related extreme precipitation events. Remarkably, northerlies from mid-high latitudes and resulting cyclonic shear in the YHRV are much greater than the composites in the study of Hsu et al. (2016) and Lee et al. (2013). So northerlies and mid-high latitude circulations system should also be emphasized when using the BSISOs to predict precipitation extremes in the YHRV.

As mentioned in Sect. 3.1, during unfavorable phases of BSISO1 (phase 6–8), there are still a few stations in southern China recording significant increases of probability for precipitation extremes. Moreover, during phase 6–8, the pattern in Yangtze River Valley is quite chaotic, with mixed signals of both insignificantly increased and decreased probability (Fig. 1f–h), rather than a regionally coherent pattern as shown in phase 2–4. Actually, composited precipitation anomalies during phase 2–4 and phase 6–8 show perfectly opposite patterns in the Yangtze River Valley (figure omitted). However, the magnitude of composited anomalies in favorable and unfavorable phases exhibits remarkable asymmetry, with reasonably strong positive anomaly and much weaker negative/insignificant anomaly. In such context, probability of extreme precipitation increased substantially during favorable phases with respect to non-BSISO days; while during unfavorable phases, the difference of probability between active and inactive BSISO1s is not that obvious. Notably, significant stations during phase 6–8 are all confined to coastal areas, where is vulnerable to tropical cyclones/typhoons. During phase 6–8, BSISO1-related circulation is coincidently manifested by an anomalous cyclone around Philippines, providing favorable background for tropical cyclone genesis and migration towards southeast coasts (Li and Zhou 2013a, b). By contrast to zonally-elongated rainband during Phase 2–4, much smaller spatial scale of both composited precipitation anomalies and precipitation extremes also indicates impacts of tropical/cyclones during phase these unfavorable phases.

Focusing on the high impact of extremes, the current study mainly evaluates the potential of BSISOs in facilitating, rather than inhibiting, multiple types of extremes. In fact, as shown in Figs. 1 and 4, in addition to significantly increased probability, there also exist significant reductions in occurrences of extremes. In general, most regions observe coordinated changes that significantly increased (decreased) occurrences of precipitation extremes correspond to significant decreases (increases) of high temperature extremes. However, during phases with well-organized cyclones in the ocean (Phase 7–8 of BSISO1, Phase 3–5 of BSISO2), even without significant increases of precipitation extremes, high temperature extremes drop significantly across central-eastern China. The anomalous easterly to the northern flank of the anomalous cyclone may be responsible for this interesting phenomenon. On one hand, it advects cold air from the sea east of the land. On the other hand, it conveys moisture to form low-based clouds, which are most effective in inhibiting incoming solar radiation (Chen et al. 2017).

This study established statistical relationship between BSISOs and simultaneous extremes, mainly based on observations. Relevant conclusions could provide some useful clues for monitoring and forecasting these high-impact weathers. Several coupled models show reasonable skills in predicting BSISO indices with lead time of 2 weeks or longer (Hsu et al. 2016). Some studies have reported that when the MJO is active, models showed higher skills in predicting wintertime extremes with longer lead time (Jones et al. 2011a, b). In favorable phases of active BSISOs, thorough evaluations on forecast skills of multiple models in the subseasonal to seasonal (S2S) database in predicting summertime simultaneous extremes in China are desirable. Our follow-up studies would conduct such evaluations. By taking advantages of excellent prediction skills of BSISO indices by models, extended-range forecasting of simultaneous extremes is promising to be fulfilled.

Acknowledgements This research was financially supported by the National Key Research and Development Program (Grant No. 2016YFA0601504(01)), Basic Research and Operation Program (Grant No. 2015Z001), and Natural Science Foundation of China (Grant No. 41575094 and Grant No. 41605029). We greatly appreciate the Editor and two anonymous reviewers for their thorough reviews and constructive comments, which help greatly improved this paper.

References

Alvarez MS, Vera CS, Kiladis GN, Liebmann B (2016) Influence of the Madden Julian Oscillation on precipitation and surface air temperature in South America. Clim Dyn 46:245–262

Annamalai H, Slingo J (2001) Active/break cycles: diagnosis of the intraseasonal variability of the Asian summer monsoon. Clim Dyn 18:85–102

Bond NA, Vecchi GA (2003) The Influence of the Madden-Julian Oscillation on Precipitation in Oregon and Washington. Weather and Forecasting 18:600–613

Chen T-C, Chen J-M (1993) The 10-20-day mode of the 1979 Indian monsoon: Its relation with the time variation of monsoon rainfall. Mon Weather Rev 121:2465–2482

Chen T-C, Chen J-M (1995) An observational study of the South China Sea monsoon during the 1979 summer: onset and life cycle. Mon Weather Rev 123:2295–2318

Chen Y, Zhai P (2013) Persistent extreme precipitation events in China during 1951–2010. Clim Res 57:143–155

Chen Y, Zhai P (2014) Two types of typical circulation pattern for persistent extreme precipitation in Central–Eastern China. Q J R Meteorol Soc 140:1467–1478

Chen Y, Zhai P (2015) Synoptic-scale precursors of the East Asia/Pacific teleconnection pattern responsible for persistent extreme precipitation in the Yangzte Rive Valley. Q J R Meteorol Soc 141:1389–1403

Chen R, Wen Z, Lu R (2016) Evolution of the circulation anomalies and the quasi-biweekly oscillations associated with extreme heat events in Southern China. J Clim 29:6909–6921

Chen Y, Zhai P, Li L (2017) Low-frequency oscillations of East Asia/Pacific teleconnection and simultaneous weather anomalies/extremes over eastern Asia. Int J Clim 37:276–295

Chu J-E, Hameed SN, Ha K-J (2012) Nonlinear, intraseasonal phases of the East Asian summer monsoon: Extraction and analysis using self-organizing maps. J Clim 25:6975–6988

Dee DP et al (2011) The ERA-Interim reanalysis: configuration and performance of the data assimilation system. Q J R Meteorol Soc 137:553–597

Ding Y, Chan JC (2005) The East Asian summer monsoon: an overview. Meteorol Atmos Phys 89:117–142

Efron B, Tibshirani RJ (1994) An introduction to the bootstrap. monographs on statistics and applied probability, vol 57. Chapman and Hall, New York

Galarneau TJ Jr, Hamill TM, Dole RM, Perlwitz J (2012) A multiscale analysis of the extreme weather events over western Russia and northern Pakistan during July 2010. Mon Weather Rev 140:1639–1664

Gao J, Lin H, You L, Chen S (2016) Monitoring early-flood season intraseasonal oscillations and persistent heavy rainfall in South China. Clim Dyn 1:1–17

Hajat S, Kovats RS, Atkinson RW, Haines A (2002) Impact of hot temperatures on death in London: a time series approach. J Epidemiol Community Health 56:367–372

Hart RE, Grumm RH (2001) Using normalized climatological anomalies to rank synoptic-scale events objectively. Mon Weather Rev 129:2426–2442

Hsu H-H, Weng C-H (2001) Northwestward propagation of the intraseasonal oscillation in the western North Pacific during the boreal summer: Structure and mechanism. J Clim 14:3834–3850

Hsu PC, Lee JY, Ha KJ (2016) Influence of boreal summer intraseasonal oscillation on rainfall extremes in southern China. Int. J Clim 36:1403–1412

Jacques-Coper M, Brönnimann S, Martius O, Vera C, Cerne B (2015a) Summer heat waves in southeastern Patagonia: an analysis of the intraseasonal timescale. Int. J Clim 36:1359–1374

Jacques-Coper M, Brönnimann S, Martius O, Vera CS, Cerne SB (2015b) Evidence for a modulation of the intraseasonal summer temperature in Eastern Patagonia by the Madden-Julian Oscillation. J Geophys Res Atmos 120:7340–7357

Jia X, Yang S (2013) Impact of the quasi-biweekly oscillation over the western North Pacific on East Asian subtropical monsoon during early summer. J Geophys Res: Atmos 118:4421–4434

Jones C, Waliser DE, Lau K, Stern W (2004a) Global occurrences of extreme precipitation and the Madden-Julian Oscillation: observations and predictability. J Clim 17:4575–4589

Jones C, Waliser DE, Lau K, Stern W (2004b) The Madden-Julian Oscillation and its impact on Northern Hemisphere weather predictability. Mon Weather Rev 132:1462–1471

Jones C, Gottschalck J, Carvalho LMV, Higgins W (2011a) Influence of the Madden-Julian oscillation on forecasts of extreme precipitation in the contiguous United States. Mont Weather Rev 139:332–350

Jones C, Carvalho LMV, Gottschalck J, Higgins W (2011b) The Madden-Julian oscillation and the relative value of deterministic forecasts of extreme precipitation in the contiguous United States. J Clim 24:2421–2428

Kalnay E, Kanamitsu M, Kistler R, Collins W, Deaven D, Gandin L, Iredell M, Saha S, White G, Woollen J (1996) The NCEP/NCAR 40-year reanalysis project. Bull Am Meteorol Soc 77:437–471

Kanamitsu M, Ebisuzaki W, Woollen J, Yang S-K, Hnilo J, Fiorino M, Potter G (2002) NCEP–DOE AMIP-II Reanalysis (R-2). Bull Am Meteorol Soc 83:1631–1643

Kuglitsch FG, Toreti A, Xoplaki E, Della-Marta PM, Zerefos CS, Türkeş M, Luterbacher J (2010) Heat wave changes in the eastern Mediterranean since 1960. Geophys Res Lett 37:1–5

Lau K, Yang G, Shen S (1988) Seasonal and intraseasonal climatology of summer monsoon rainfall over Eeat Asia. Mon Weather Rev 116:18–37

Lee JY, Wang B, Wheeler MC, Fu XH, Waliser DE, Kang I-S (2013) Real-time multivariate indices for the boreal summer intraseasonal oscillation over the Asian summer monsoon region. Clim Dyn 40:493–509

Lee S-S, Wang B, Waliser DE, Neena JM, Lee J-Y (2015) Predictability and prediction skill of the boreal summer intraseasonal oscillation in the Intraseasonal Variability Hindcast Experiment. Clim Dyn 45:2123–2135

Li R, Zhou W (2013a) Modulation of western North Pacific tropical cyclone activity by the ISO. Part one: Genesis and intensity. J Clim 26:2904–2918

Li R, Zhou W (2013b) Modulation of western North Pacific tropical cyclone activity by the ISO. Part two: tracks and landfalls. J Clim 26:2919–2930

Li J, Mao J, Wu G (2015) A case study of the impact of boreal summer intraseasonal oscillations on Yangtze rainfall. Clim Dyn 44:2683–2702

Liu H-B, Yang J, Zhang D-L, Wang B (2014) Roles of synoptic to quasi-biweekly disturbances in generating the summer 2003 heavy rainfall in East China. Mon Weather Rev 142:886–904

Lu R, Dong H, Su Q, Ding H (2014) The 30–60-day intraseasonal oscillations over the subtropical western North Pacific during the summer of 1998. Adv Atmos Sci 31:1–7

Madden RA (1986) Seasonal variations of the 40–50 day oscillation in the tropics. J Atmos Sci 43:3138–3158

Madden RA, Julian PR (1971) Detection of a 40–50 day oscillation in the zonal wind in the tropical Pacific. J Atmos Sci 28:702–708

Madden RA, Julian PR (1972) Description of global-scale circulation cells in the tropics with a 40–50 day period. J Atmos Sci 29:1109–1123

Madden RA, Julian PR (1994) Observations of the 40-50-day tropical oscillation-A review. Mon Weather Rev 122:814–837

Mao J, Chan JC (2005) Intraseasonal variability of the South China Sea summer monsoon. J Clim 18:2388–2402

Mao J, Sun Z, Wu G (2010) 20–50-day oscillation of summer Yangtze rainfall in response to intraseasonal variations in the subtropical high over the western North Pacific and South China Sea. Clim Dyn 34:747–761

Matsueda S, Takaya Y (2015) The Global Influence of the Madden–Julian Oscillation on Extreme Temperature Events. J Clim 28:4141–4151

Matthews AJ (2004) Intraseasonal variability over tropical Africa during northern summer. J Clim 17:2427–2440

Oh H, Ha K-J (2015) Thermodynamic characteristics and responses to ENSO of dominant intraseasonal modes in the East Asian summer monsoon. Clim Dyn 44:1751–1766

Pullen J, Gordon AL, Flatau M, Doyle JD, Villanoy C, Cabrera O (2015) Multiscale influences on extreme winter rainfall in the Philippines. J Geophys Res Atmos 120:3292–3309

Ren X, Yang X-Q, Sun X (2013) Zonal oscillation of western Pacific subtropical high and subseasonal SST variations during Yangtze persistent heavy rainfall events. J Clim 26:8929–8946

Sun Y, Zhang X, Zwiers FW, Song L, Wan H, Hu T, Yin H, Ren G (2014) Rapid increase in the risk of extreme summer heat in Eastern China. Nat Clim Change 4:1082–1085

Tencer B, Weaver A, Zwiers F (2014) Joint occurrence of daily temperature and precipitation extreme events over Canada. J Appl Meteorol Clim 53:2148–2162

Tsou C-H, Hsu P-C, Kau W-S, Hsu H-H (2005) Northward and northwestward propagation of 30–60 day oscillation in the tropical and extratropical western North Pacific. J Meteorol Soc Japan 83:711–726

Waliser DE (2006) Intraseasonal variability. In: The Asian Monsoon. Springer

Wang B, Rui H (1990) Synoptic climatology of transient tropical intraseasonal convection anomalies: 1975–1985. Meteorol Atmos Phys 44:43–61

Wang W, Zhou W, Li X, Wang X, Wang D (2016) Synoptic-scale characteristics and atmospheric controls of summer heat waves in China. Clim Dyn 46:2923–2941

Welch BL (1947) The generalization ofstudent's' problem when several different population variances are involved. Biometrika 34:28–35

Wheeler MC, Hendon HH (2004) An all-season real-time multivariate MJO index: Development of an index for monitoring and prediction. Mon Weather Rev 132:1917–1932

Yang J, Wang B, Bao Q (2010) Biweekly and 21-30-day variations of the subtropical summer monsoon rainfall over the lower reach of the Yangtze River basin. J Clim 23:1146–1159

Zhang C (2005) Madden-julian oscillation. Rev Geophys 43:RG2003. doi:10.1029/2004RG000158

Zhang X, Alexander L, Hegerl GC, Jones P, Tank AK, Peterson TC, Trewin B, Zwiers FW (2011) Indices for monitoring changes in extremes based on daily temperature and precipitation data. Wiley interdisciplinary reviews. Clim Change 2:851–870

Zhou W, Chan JC (2005) Intraseasonal oscillations and the South China Sea summer monsoon onset. Int. J Clim 25:1585–1609

Zhu C, Nakazawa T, Li J, Chen L (2003) The 30–60 day intraseasonal oscillation over the western North Pacific Ocean and its impacts on summer flooding in China during 1998. Geophys Res Lett 30 doi:10.1029/2003GL017817